Formation and Spectroscopy of Dicyanotriacetylene (NC 8 N) in Solid Kr

ARTICLE *in* THE JOURNAL OF PHYSICAL CHEMISTRY A · NOVEMBER 2014

Impact Factor: 2.69 · DOI: 10.1021/jp509908z · Source: PubMed

THE JOURNAL OF PHYSICAL CHEMISTRY A

Article

pubs.acs.org/JPCA

Formation and Spectroscopy of Dicyanotriacetylene (NC_8N) in Solid Kr

Michał Turowski,*[,†] Claudine Crépin,[‡] Stéphane Douin,[‡] and Robert Kołos[†]

[†]Institute of Physical Chemistry of the Polish Academy of Sciences, Kasprzaka 44/52, 01-224 Warsaw, Poland

[‡]Institut des Sciences Moléculaires d'Orsay, UMR 8214 CNRS, Université Paris-Sud, 91405 Orsay, France

Supporting Information

ABSTRACT: Thermally induced creation of dicyanotriacetylene (NC_8N) was observed in solid krypton. Samples were obtained by cryogenic trapping of gaseous cyanoacetylene/Kr mixtures subjected to electric discharges. Strong a $^3\Sigma^+_u \rightarrow X\ ^1\Sigma^+_g$ phosphorescence of NC_8N is reported here for the first time; its vibronic structure permitted the measurement of several ground-state vibrational frequencies. Other chemical species, mostly smaller than the precursor molecule, have also been formed, among them the dicarbon molecule (C_2), and these may serve as indispensable building blocks in the NC_8N synthesis. Processes leading to the elongation of cyanoacetylenic chains are of potential importance for the chemistry of icy grains present in the interstellar gas clouds.

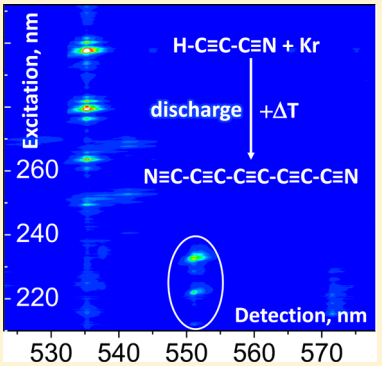

1. INTRODUCTION

Cyanopolyynes are of significant astrophysical importance due to their presence in inter- and circumstellar environments,[1−4] extragalactic sources,[5] and cometary atmospheres[6] or in the atmosphere of Saturn's moon Titan.[7] $HC_{11}N$ is the largest interstellar molecule of this series detected thus far.[8] The radio astronomical identification of dicyanoacetylenes (NC_nN, $n = 2, 4, 6, ...$) which lack a permanent electric dipole moment, is not possible. During the Voyager and Cassini−Huygens missions, NC_2N and NC_4N have, however, been detected in Titan's atmosphere with mass spectrometry[9] and with far-IR instruments.[7,10] It is generally recognized that apart from gas-phase reactions, the interstellar formation of complex molecules may occur within icy shells of mineral dust particles.

Gas-phase chain growth processes leading to polyacetylenes were studied by Seki et al.[11] The formation of several mono- and dicyanopolyynes in rare gas (Rg) matrixes, has been reported over the last several years. HC_5N and HC_7N were synthesized in solid Ar, starting from isolated, UV-irradiated intermolecular complexes, HC_3N:HC_2H and HC_5N:HC_2H, respectively, and detected via both IR absorption and optical phosphorescence.[12,13] The formation of HC_5N, NC_4N, and NC_6N in low temperature Ar and Kr matrixes was proved (by electronic luminescence measurements) to occur also in UV-photochemical Rg-matrix experiments involving HC_3N as the sole precursor.[14] Similar long-chain carbon cluster formation processes have been studied by Wu et al.,[15] who employed VUV photolysis of acetylene embedded in a neon matrix and observed IR absorption of bare C_n ($n = 3−12$) chains, together with C_2H, C_2H_3, C_4H, HC_4H, C_8H^-, and HC_8H. The laser-induced fluorescence spectra of HC_5N^+, HC_7N^+, NC_4N^+, NC_6N^+, and NC_8N^+ have been previously reported.[16−19] The cations were created in a self-igniting pulsed dc discharge in contact with HC_3N:Ne gas mixtures and trapped in solid Ne. These experiments, though focused on ions, have suggested the parallel presence of respective neutral products.

Grösser and Hirsch[20] and Schermann et al.[21] reported on the extraction of NC_8N from a solid deposit formed in a fullerene-synthesis reactor, in which cyanogen (NC_2N) reacted with graphite vapors. The corresponding UV absorption spectrum of a liquid solution and IR absorption of the compound dispersed in solid NaCl have been measured. Cataldo et al.[24] have detected NC_8N in a mixture obtained with prolonged electrical discharges between graphite electrodes immersed in liquid nitrogen. The fully allowed electronic absorption of the molecules NC_nN ($n = 6, 8, 10$)[22,23] and HC_nN ($n = 7, 9, 11, 13, 15$) in organic solvents was described.

Here, we show evidence for NC_8N formation in thermally processed (annealed) HC_3N:Kr solid samples prepared using the cold window radial discharge (CWRD) technique.[25] Experimental data describing the newly discovered luminescence of NC_8N and the ensuing ground-state vibrational frequencies are presented. Results concerning several additional products are also reported.

2. EXPERIMENTAL SECTION

Experiments were conducted in Warsaw and in Orsay. HC_3N was synthesized using a slightly modified version of the Miller

Special Issue: Markku Räsänen Festschrift

Received: September 30, 2014
Revised: November 13, 2014

   dx.doi.org/10.1021/jp509908z | J. Phys. Chem. A XXXX, XXX, XXX−XXX

and Lemmon method.[26] To obtain ^{15}N-labeled cyanoacetylene, isotopically enriched ammonia (obtained from $^{15}NH_4Cl$; Spectra Stable Isotopes, isotopic purity 99%) was used.[27] Cryogenic samples were prepared by mixing the host gas (krypton, Messer Group GmbH, purity 4.0) with cyanoacetylene vapors at a ratio between 1:1000 and 1:500, and by subsequently solidifying the mixture onto a synthetic sapphire cold window cooled within an Air Products *Displex* closed cycle cryostat, either DE 202 FF (Orsay) or DE 202S (Warsaw), with the lowest attained temperatures of about 8 and 15 K, respectively. In Orsay, the experiments were carried out at *Centre Laser de l'Université Paris-Sud* where a variety of pulsed tunable sources (optical parametric oscillators and dye lasers) was available. Luminescence, dispersed with a 0.3 m Acton SpectraPro 2300i grating monochromator (ca. 0.08 nm resolution), was recorded with a CCD camera (Andor DH720). The dispersed luminescence as well as luminescence excitation spectra of previously created products were mainly measured with a laser source (consisting of an optical parametric amplifier and the second harmonic generation system EKSPLA-PG411 pumped with a mode-locked picosecond Nd:YAG laser EKSPLA-SL300) providing the radiation tunable within the 210−340 nm range (bandwidth ∼10 cm^{-1}; wavelength calibration accuracy ∼1 nm). Emission spectra were corrected neither for the sensitivity of the detection system nor for the instabilities of the laser fluence. The luminescence lifetime was determined in pulse excitation experiments with the gated CCD camera used for the analysis of dispersed luminescence. For UV absorption measurements, either the above-described CCD-based setup with a deuterium lamp as a broadband UV source (Orsay) or a digitalized Cary-17 spectrometer featuring a Hamamatsu R 955 photomultiplier and a photon-counting system (Warsaw) was employed. For IR absorption measurements, a Nicolet 160 SX spectrometer with a liquid nitrogen cooled InSb detector was used. The usual resolution of the spectra, resultant from the averaging of not less than 1024 interferograms, was 0.5 cm^{-1}. A high pressure Xe lamp was used for "photobleaching", monitored via UV and IR absorption spectroscopy (Warsaw).

The cold window radial discharge (CWRD) technique has been previously described.[25] Shortly, high voltage is applied to a stainless electrode, the tip of which is placed in the center of the cold deposition window within the cryostat. The circular window holder, made of copper, is grounded. Once an effusion beam of the gaseous mixture arrives in the vicinity of the cold surface, it is subjected to a glow discharge, just before being solidified at the surface. The technique has been successfully used, e.g., as a source of HNCCC starting from HC_3N precursor,[28] and recently as a new method for synthesis of rare gas inclusion species, namely, $HKrC_3N$ and $HKrC_5N$.[29]

3. COMPUTATIONAL METHODS

All calculations were carried out using the GAUSSIAN 03 program package.[30] IR absorption intensities and Raman activities were obtained with a density functional theory (DFT) calculations using the Becke's three-term correlation functional and the exchange functional of Perdew and Wang 1991 (B3PW91).[31−35] The augmented version of the triple-ζ Dunning-type basis set (aug-cc-pVTZ) was used. Vibrational frequencies were calculated with the harmonic approximation, and scaled with the factor of 0.96.[36,37] Default convergence criteria of the GAUSSIAN software were applied for all computations.

4. RESULTS AND DISCUSSION

In previous experiments, the cryogenic trapping of an HC_3N/Rg mixture subjected to the CWRD treatment has led to several HC_3N-related species, including the isomers HC_2NC,[38,39] HNC_3,[28,39] and HCNCC,[39,40] the C_3N^- anion,[41,42] and $HKrC_3N$,[29] all of which were detected via IR absorption spectroscopy. In the present work, the occurrence of various products was mostly revealed due to their electronic emission. Rich luminescence spectra were detected during the cryogenic trapping of gas mixtures, accompanied by electric discharges. UV laser irradiation could then be used to induce luminescence in a CWRD-prepared sample; a number of UV and visible product bands have consequently been identified. Moreover, new bands appeared upon the thermal annealing. Figure 1 shows an example

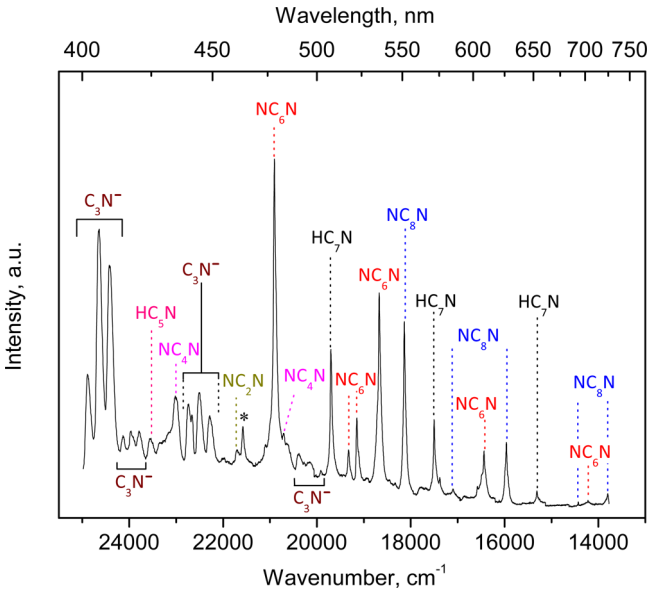

Figure 1. Long-lived (longer than 1 μs) luminescence excited at 220.8 nm, from a HC_3N/Kr matrix deposited with CWRD discharges. Spectrum recorded after the thermal annealing at 35 K, followed by recooling to 13 K. Several bands remain unidentified, the strongest one (at 21 578 cm^{-1}) is asterisked.

of electronic emission spectrally resolved in a broad frequency range. Some prominently appearing products have been easily identified, due to their already known luminescent properties. Nevertheless, careful examination of 3-dimensional graphs (3D spectra) depicting long-lived luminescence intensity as a function of both excitation and detection wavelengths (Figure 2) has revealed some emission features that have not been previously observed for UV-irradiated HC_3N/Rg solids.[14] These bands are the main focus of the present paper.

4.1. NC_8N Identification. Formerly measured phosphorescence spectra of C_3N^-,[42] HC_5N,[43] NC_2N,[44] NC_4N,[45,46] and NC_6N[14] have allowed for straightforward identification of these species in our spectra, together with HC_7N (cyanotriacetylene), the strong phosphorescence of which has been very recently discovered.[13] All these emissions are dominated by a vibronic progression with a characteristic spacing of approximately 2100 cm^{-1}. A new progression with similar characteristics appeared in our experiments; this well-defined set of long-lived (τ > 1 μs) emission bands, formerly never reported, became discernible following the selective excitation (at approximately 233 nm) of a previously annealed sample. The said emission system (Figure 3)

dx.doi.org/10.1021/jp509908z | J. Phys. Chem. A XXXX, XXX, XXX−XXX

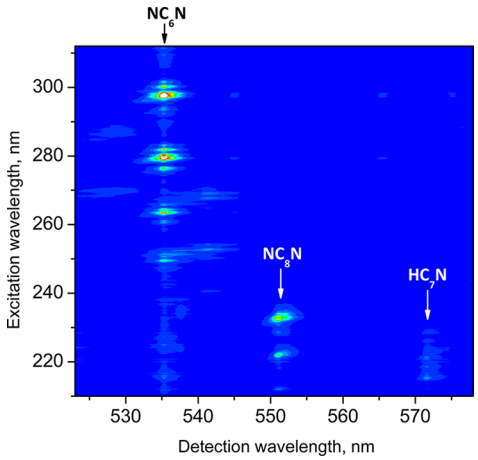

Figure 2. Three-dimensional (excitation−detection−intensity) graph for phosphorescence emitted from a HC_3N:Kr matrix prepared with the CWRD technique. Spectrum recorded after the thermal annealing (warm-up to 35 K, followed by the recooling to 13 K). A 1:1 mixture of ^{14}N- and ^{15}N-isotopologues of HC_3N has been used.

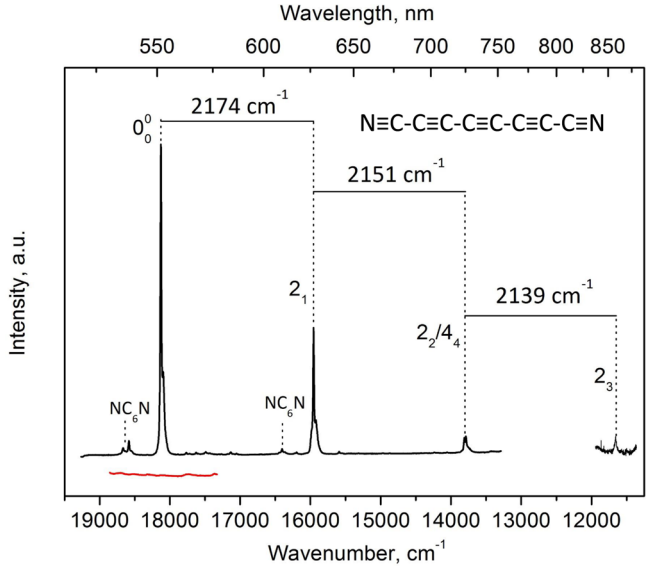

Figure 3. Phosphorescence assigned to NC_8N molecules isolated in solid krypton. Spectrum results from the horizontal cut, at 233 nm, of the graph presented in Figure 2. The intensity of the 2_3 band is 10-fold expanded. The short bottom trace (in red, around 18 000 cm^{-1}, 5-fold intensity expansion) shows the emission signal measured before the thermal annealing.

was slightly contaminated with known[14] NC_6N phosphorescence bands. The first (apparently 0−0) band of the progression appears at 18 135 cm^{-1} (551 nm), separated by 2175 cm^{-1} from the next strong vibronic band (the value of 2174 cm^{-1}, was measured for a mixture of ^{14}N- and ^{15}N-isotopologues). The corresponding excitation spectrum, extracted from the 3D graphs of Figure 2, is shown in the top panel of Figure 4. It features a distinct vibronic progression with maxima at 232.7, 222, and 211 nm.

These data, combined with the absorption spectra published by Grösser and Hirsch,[20] Schermann et al.,[21] and Cataldo[23] for *n*-hexane, acetonitrile, and *n*-octane solutions, respectively, suggested NC_8N as the species responsible for the new phosphorescence. Indeed, the vibronic structure of our phosphorescence excitation spectrum matches (neglecting the

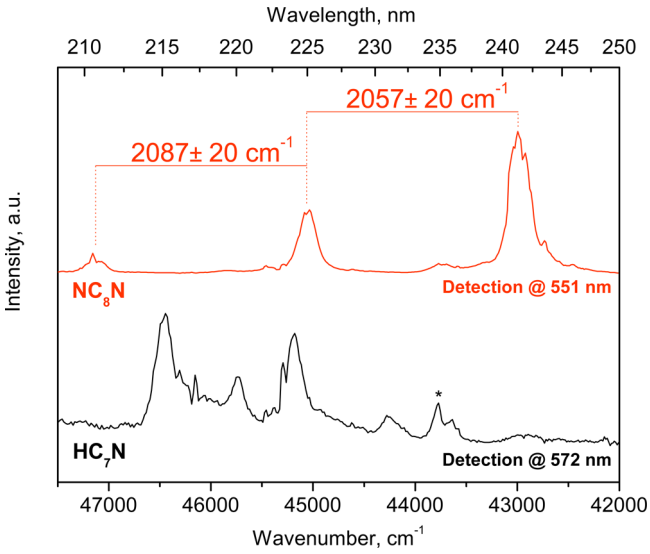

Figure 4. Phosphorescence excitation spectra assigned to NC_8N (top) and to HC_7N (bottom). Traces obtained by the vertical cuts of the graph presented in Figure 2. The asterisked band belongs to an as yet unidentified product.

inevitable solvent shifts) that reported for the UV absorption. The excitation wavelength of 233 nm corresponds to the intense transition of an allowed system, most likely $^1\Sigma_u^+ \leftarrow {}^1\Sigma_g^+$. As illustrated by Figure 3, the bands assigned to NC_8N appeared only after the annealing of CWRD-deposited HC_3N:Kr matrixes. This points to the role of thermally induced mobility of photolysis products in the formation of a long, rod-like species.

Moreover, the singlet−triplet splitting predicted for NC_8N with DFT (B3PW91/aug-cc-pVTZ), 2.02 eV, matches reasonably well the experimental value indicated by the phosphorescence: 2.25 eV. Calculations of vertical singlet−singlet electronic transitions, performed at the TD B3PW91/aug-cc-pVTZ level for the first 20 excited singlet states of NC_8N, indicate the presence of two weak electronic systems (predicted oscillator strengths $f < 10^{-3}$), at about 3.0 eV (410 nm) and 4.9 eV (350 nm), the identity of which should be $A\ ^1\Sigma_u^- - X\ ^1\Sigma_g^+$ and $B\ ^1\Delta_u - X\ ^1\Sigma_g^+$, respectively, based on the analogy with NC_2N, NC_4N, or NC_6N spectroscopy.[47−50] Next, a very strongly allowed ($f = 4.5$) HOMO−LUMO ($\pi-\pi^*$) system, most likely $C\ ^1\Sigma_u^+ \leftarrow X\ ^1\Sigma_g^+$, is expected around 5.1 eV (240 nm), fitting well to the position of the first absorption band (233 nm) of the progression assigned to NC_8N in the phosphorescence excitation spectrum (Figure 4).

The assignment of the new electronic system to NC_8N is justified not only because of the above presented arguments but also in view of the fact that similar centrosymmetric cyanopolyynes (NC_4N, NC_6N) have already been shown to form from the same precursor, i.e., from HC_3N. An additional proof came from the plot (Figure 5) depicting the wavelength positions of the vibrationless origin (0−0 band) for a $^3\Sigma_u^+ - X\ ^1\Sigma_g^+$ phosphorescence, as a function of NC_nN chain size (the analogous data are also presented for a $^3\Sigma^+ - X\ ^1\Sigma^+$ phosphorescence of monocyanopolyynes, HC_nN). The new entry, corresponding to NC_8N, clearly follows a general linear trend.

The frequencies of NC_8N g-symmetry vibrational modes, derived from the analysis of well-resolved phosphorescence bands, agree fairly well with DFT-obtained values. These are reported in Table 1. Our calculations correctly predict also the u-

dx.doi.org/10.1021/jp509908z | J. Phys. Chem. A XXXX, XXX, XXX−XXX

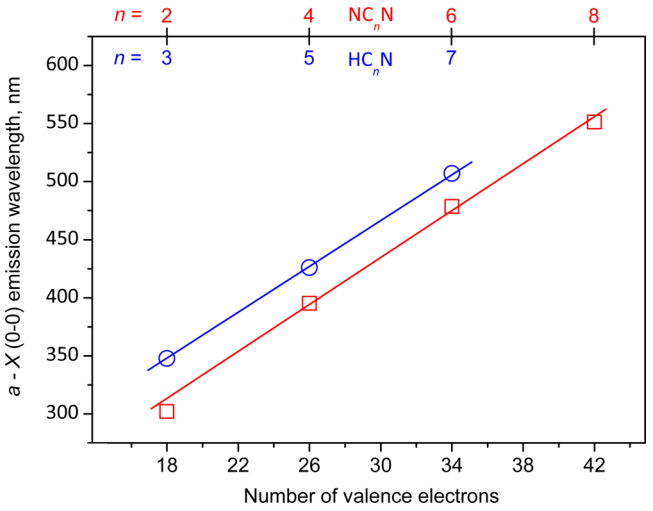

Figure 5. Squares: vibrationless origin (0−0 band) wavelengths corresponding to the a $^3\Sigma_u^+ - X\ ^1\Sigma_g^+$ phosphorescence, plotted vs the number of valence electrons or vs the number of carbon atoms. Circles: the analogous data, after Couturier-Tamburelli et al.,[13] characterizing the a $^3\Sigma^+ - X\ ^1\Sigma^+$ phosphorescence of C_3N^-, HC_5N, and HC_7N (the linear C_3N^- anion is used in place of the isoelectronic, yet nonphosphorescent HC_3N molecule. Lines depict the least-squares linear fitting to experimental data.

symmetry modes formerly observed by Grösser and Hirsch[20] via IR absorption of solid NC_8N dispersed in NaCl (Table 1).

In experiments with a 1:1 mixture of $HC_3{}^{15}N$ and $HC_3{}^{14}N$, the weakness of isotopic effects and/or the limited resolving power of our luminescence detection system did not permit us to distinguish individual signals coming from $^{14}NC_8{}^{14}N$, $^{14}NC_8{}^{15}N$, and $^{15}NC_8{}^{15}N$ isotopologues; it was, however, possible (see below), to discern some changes when comparing certain maxima of NC_8N bands produced with ^{15}N-enriched and isotopically pure $HC_3{}^{14}N$ precursors.

Table 2 lists the assignments of the observed phosphorescence bands. The main bands are marked in Figure 3 (see Figure S1 of Supporting Information for the detailed picture). The well-resolved doublet in the vicinity of 13 800 cm^{-1} (Figure 3, Figure S2 (Supporting Information)) may result from a Fermi resonance between $2\nu_2$ and $4\nu_4$. The theoretical approach employed in this study does not allow for a reliable reproduction of anharmonic interactions between excited vibrational levels. Present calculations have predicted a resonance (which was not experimentally found to occur) between the fundamental mode ν_2 and the first overtone $2\nu_4$; it can nevertheless be speculated that the necessary frequency-match condition is in fact satisfied for higher vibrational excitation (resonances of that type were recently observed in the vibronic structure of NC_4N phosphorescence[46]). In our experiment with the isotopically labeled precursor, the doublet was still present (its splitting being slightly altered: from the value of 24 cm^{-1} for $HC_3{}^{14}N$ to 21 cm^{-1} for a 1:1 mixture of ^{14}N- and ^{15}N-containing precursors), with the relative intensity of its components reversed (Figure S2, Supporting Information). This behavior plausibly reflects the susceptibility of Fermi resonance conditions to minute changes in harmonic ν_2 and ν_4 frequencies introduced by the increased mass of the nitrogen atom (the currently predicted changes are only −4 and less than −1 cm^{-1}, for ν_4 and ν_2, respectively).

Another observation supporting the assignment of the discussed phosphorescence to NC_8N comes from the identity of the mode responsible for the main vibronic progression. This progression, in the known cases of other dicyanoacetylenes studied in solid krypton, is governed by a symmetric mode having the highest Raman scattering activity. This is true for NC_2N (ν_1 =

Table 1. Vibrational Spectroscopy of NC_8N in the Ground Electronic State, As Predicted Theoretically and As Revealed by Electronic Phosphorescence

	theory					Kr matrix		
		isotopic shifts (cm^{-1})[a]						
mode	freq (cm^{-1}) $^{14}NC_8{}^{14}N$	$^{15}NC_8{}^{15}N$	$^{14}NC_8{}^{15}N$	IR intensity, (km/mol)	Raman activity	freq (cm^{-1}) from $HC_3{}^{14}N$ precursor	freq (cm^{-1}) from mixed $HC_3{}^{14}N$ and $HC_3{}^{15}N$ precursors	relative intensity
ν_1 (σ_g)	2245	−17	−10	0	4507			
ν_2 (σ_g)	2166	0	0	0	26469	2175	2174	vs
ν_3 (σ_g)	2079	−9	−5	0	138		2082[b,c]	vvw
ν_4 (σ_g)	1068	−8	−4	0	35		1079[c]	w
ν_5 (σ_g)	373	−6	−3	0	1	365	365	w
ν_6 (σ_u)	2260	0	−3	154	0	[2247][d]		
ν_7 (σ_u)	2166	−17	−8	0	0	[2187][d]		
ν_8 (σ_u)	1365	−4	−2	0	0			
ν_9 (σ_u)	730	−9	−4	1	0			
ν_{10} (π_g)	660	0	0	0	39	640	640	w
ν_{11} (π_g)	513	−1	−1	0	7	501	503	w
ν_{12} (π_g)	309	−1	0	0	0			
ν_{13} (π_g)	108	−1	−1	0	0			
ν_{14} (π_u)	563	0	0	3	0			
ν_{15} (π_u)	460	−1	−1	6	0			
ν_{16} (π_u)	201	−1	−1	7	0			
ν_{17} (π_u)	40	−1	0	4	0			

[a]Frequency shift with respect to $^{14}NC_8{}^{14}N$ isotopologue. [b]Very weak feature observed on the slope of the 2_1 band. [c]Features seen only for the experiment with $HC_3{}^{14}N$:$HC_3{}^{15}N$ mixture of precursors where the better S/N ratio has been obtained. [d]IR absorption data for solid NC_8N dispersed in NaCl.[20] Another frequency reported in ref 20, 2120 cm^{-1}, may originate from a combination mode or from a Fermi resonance pair.

dx.doi.org/10.1021/jp509908z | J. Phys. Chem. A XXXX, XXX, XXX−XXX

Table 2. Vibronic Assignments for the a $^3\Sigma_u^+ \rightarrow X\ ^1\Sigma_g^+$ System of NC_8N, Detected in Cyanoacetylene-Doped, CWRD-Deposited, and Subsequently Annealed Kr Matrixes

from $HC_3{}^{14}N$			from $HC_3{}^{14}N + HC_3{}^{15}N$					
ν (cm^{-1})	λ (nm)	$\Delta\nu^a$ (cm^{-1})	ν (cm^{-1})	λ (nm)	$\Delta\nu^a$ (cm^{-1})	intensity	isotopic shift^b (cm^{-1})	assignment
18135	**551.43**	**0**	**18129**	**551.60**	**0**	**vs**	**0**	0_0
			18093	552.70	36			site
17897		238	17884	559.16	245	vvw	+7	16_117_1
17770		365	17764	562.94	365	w	0	5_1
17734		401	17720	564.33	409	vw	+8	$12_113_1{}^c$
17637		501	17626	567.34	503	w	+2	11_1
17634								
			17596	568.30	533	vw		$15_117_1{}^c$
17495		640	17489	571.79	640	w	0	10_1
			17297	578.12	832	vw		11_112_1
			17266	579.18	863	vw		5_111_1
			17132	583.70	997	w		5_112_2
			17050	586.50	1079	w		4_1
			16197	617.40	1932	w		10_3
15960	**626.58**	**2175**	**15955**	**626.76**	**2174**	**s**	**−1**	2_1
			15923	628.02	32	ms		site
			15708	636.62	247	vvw		$2_116_117_1$
15596	641.20	364	15593	641.31	362	w	−2	2_15_1
			15549	643.13	406	vvw		$2_112_113_1{}^c$
15455	647.02	504	15455	647.04	500	vww	−4	2_111_1
15311	653.14	649	15315	652.95	640	vvw	−9	2_110_1
			14970	668.00	985	vvw		$2_15_112_2$
			14871	672.47	1085	vvw		2_14_1
			14054	711.52	1901	vw		2_110_3
	724.23	2152	13810	724.11	2145	mw	−7	4_4
	725.50	2176	13789	725.22	2166	mw	−10	2_2
			11656	857.93	2133	w		2_3

^{a}Frequency decrease, relative to the preceding (bolded) band of the main vibronic progression. ^{b}Difference between vibronic spacings $\Delta\nu$, listed in the preceding columns. ^{c}Tentative assignments.

2332 cm^{-1}),[44,51,52] NC_4N (ν_1 = 2294 cm^{-1}),[10,45,46] and NC_6N (ν_2 = 2237 cm^{-1})[14,52] (the selection rules for a $^3\Sigma_u^+ \leftarrow X\ ^1\Sigma_g^+$ phosphorescence, originating from the vibrationless a state, allow only for the transitions involving g-symmetry (i.e., Raman-active) X-state vibrations). For NC_8N, calculations indicate the ν_2 stretching fundamental to be by far the most active Raman mode (cf. Table 1). Its calculated frequency (2166 cm^{-1}) is in acceptable agreement with the observed vibronic spacing of 2175 cm^{-1}.

Vibrational frequencies in the excited $^1\Sigma_u^+$ state (Table 3), derived following the optimization of its geometry, also deserve a comment. The main vibrational progression of the excitation spectrum (see Figure 4 for the vibronic spacing) is most likely governed by the ν_2 mode of the $^1\Sigma_u^+$ state; normal coordinate analysis reveals its close similarity to the above-discussed ν_2 mode of the ground electronic state. Calculated differences between ground- and excited-state ν_2 frequencies are similar to those observed.

Table 3. Vibrational Spectroscopy of NC_8N in the Excited $^1\Sigma_u^+$ State (ca. 5.1 eV above the Ground State), As Derived with TD B3PW91/aug-cc-pVTZ Calculations (Frequencies (cm^{-1}) Scaled with a Factor of 0.96)

mode	frequency	mode	frequency
ν_1 (σ_g)	2148	ν_{10} (π_g)	511
ν_2 (σ_g)	2030	ν_{11} (π_g)	428
ν_3 (σ_g)	1894	ν_{12} (π_g)	209
ν_4 (σ_g)	1086	ν_{13} (π_g)	47
ν_5 (σ_g)	373	ν_{14} (π_u)	585
ν_6 (σ_u)	2128	ν_{15} (π_u)	469
ν_7 (σ_u)	1975	ν_{16} (π_u)	303
ν_8 (σ_u)	1376	ν_{17} (π_u)	102
ν_9 (σ_u)	734		

The above-mentioned vibronic spacing of approximately 2060 cm^{-1} can be compared to those governing the main vibrational progressions in gas-phase $^1\Sigma_u^+ - {}^1\Sigma_g^+$ UV absorption spectra of NC_6N (2100 cm^{-1}) and NC_4N (2150 cm^{-1}).[48] Former low resolution measurements of the NC_8N absorption spectrum in *n*-hexane given by Groesser and Hirsch[20] and Cataldo[23] indicate spacing of similar magnitude, respectively 2008 and 2024 cm^{-1}.

4.2. Additional Products. *4.2.1. Previously Identified Cyanopolyynes.* As mentioned before, strong luminescence coming from C_3N^-, HC_5N, NC_2N, NC_4N, NC_6N, and HC_7N was easily recognized. Additionally, new spectral assignments have been made for some of these molecules. In the case of a $^3\Sigma^+ - X\ ^1\Sigma^+$ phosphorescence of C_3N^-, we could identify three weak bands in the vicinity of 20 400 cm^{-1} (490 nm), not referred to by Turowski et al.:[42] 1_22_2 (at 20 622 ± 30 cm^{-1}, on the slope of an intense NC_6N band), 1_32_1 (20 383 cm^{-1}), and 1_4 (20 146 cm^{-1}).

In the case of HC_7N (this species, just like NC_8N, appearing only for an annealed matrix), the analysis of 3D excitation−emission graphs permitted us to extract the phosphorescence excitation spectrum in the 210−240 nm range, shown in Figure 4.

dx.doi.org/10.1021/jp509908z | J. Phys. Chem. A XXXX, XXX, XXX−XXX

The most intense band, around 215 nm, is in reasonable agreement with the previously reported UV absorption of HC_7N in liquid solutions.[24,53] An in-depth analysis of this phosphorescence excitation spectrum is under progress.

4.2.2. Carbon Molecules and Small Fragments. Apart from above-mentioned photolysis products, small molecular fragments were detected. Swan system fluorescence ($d\ ^3\Pi_g \leftarrow a\ ^3\Pi_u$) of C_2 was especially well observed; the bands at 470, 509, and 553 nm, matching those reported by Frosch et al.,[54] appeared in the light emitted by the matrix during the CWRD deposition, as well as in laser-excited luminescence from a cryogenic sample prepared with the CWRD technique (Figure 6). The bottom

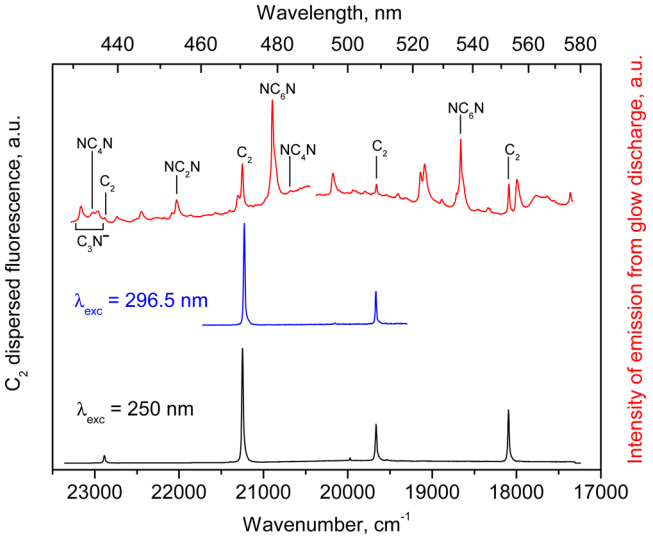

Figure 6. Bottom and middle traces: $d\ ^3\Pi_g \leftarrow a\ ^3\Pi_u$ fluorescence (Swan system) of C_2, selectively excited in a CWRD-deposited HC_3N/Kr sample (four strongest features are the first bands of the $v' = 2$ progression). Upper trace: spectrum of a glow accompanying electric discharges (CWRD) during the HC_3N/Kr matrix deposition.

trace of Figure 6 presents the Swan bands observed following the excitation with quanta corresponding to the Mulliken system D $^1\Sigma_u^+ \leftarrow X\ ^1\Sigma_g^+$ at 250 nm. The respective absorption band was reported, for solid Kr, at 248 nm.[55] Interestingly, the Swan fluorescence turned out to be selectively excited also at the wavelength of 296.5 nm; it corresponds, most likely, to a weakly bound chemical species transformed, upon the absorption of mid-UV photons, into electronically excited C_2. This point deserves further studies.

If C_2 is produced and becomes mobile in the matrix during annealing, the assembly of other species, such as tetracarbon (C_4), can be expected. On the basis of a UV−vis absorption study by Freivogel et al.,[56] two fairly weak features in our UV absorption spectra, at 370.2 and 356.6 nm in Kr, may possibly correspond to the ones of linear C_4, reportedly found for solid Ne at 367.3/369.5 nm (double band) and 355.3 nm by Freivogel et al.[56] These spectral features have, however, not been considerably affected by annealing or by photobleaching of the sample suggesting, if the assignment is true, that the coupling of two C_2 molecules does not significantly compete with other reactions of C_2, in particular with the production of longer cyanoacetylenes. The IR absorption bands of C_4, at 1539.5 cm^{-1} in Kr[57] and at 170 cm^{-1} in Ar,[58] were out of our detection range (limited by the substrate window made of sapphire).

Similar to C_4, the presence of C_3 (marked with visible phosphorescence[59] and IR absorption[57,60]) is not excluded, yet not sufficiently confirmed. A phosphorescence band was detected at 593.5 nm, most likely assignable to the vibrationless origin of the $a\ ^3\Pi_u \rightarrow X\ ^1\Sigma_g^+$ transition observed at 590.7 nm in Ne matrix by Čermák et al.[59] As reported by Weltner and McLeod,[61] the excitation wavelength for this emission, 407 nm, coincided with an intense absorption band of C_3; the latter was, however, not detectable in our optical absorption spectra.

We have tentatively identified C_2H via its broad visible fluorescence. This quasi-continuous emission was first observed by Okabe et al.[62] in the 400−550 nm range, following the VUV photolysis of C_2H_2 or BrC_2H, and was assigned to the $A\ ^2\Pi \leftarrow X\ ^2\Sigma^+$ transition of C_2H.[63] The shape of this fluorescence varies; Boyé et al.[64] observed its evolution (in the 400−900 nm range) when the amount of energy deposited in the excited radical was systematically changed.

We have not found any spectral signatures of C_3H or C_4H. The presence of CH was indicated by strong A−X (0−0), B−X (0−0), and B−X (0−1) fluorescence bands at, respectively, 434, 394, and 442 nm. These emissions, excited at 388 nm, are in good agreement with the spectrum of CH generated in solid Kr from methane.[65]

CN radicals were also clearly detected via the strong $B\ ^2\Sigma^+ \leftarrow X\ ^2\Sigma^+$ (0−0) absorption band at 387.4 nm, corresponding to the one (388.4 nm) observed by Milligan and Jacox[66] following the HCN photolysis in solid Ar. The electronic absorption of CN strongly increased following the photobleaching, in parallel with the decrease of IR absorption at 2019 cm^{-1}, assigned[39] to the CN^- anion (the gas-phase electron affinity of CN^- was reported as 3.862 eV, corresponding to approximately 321 nm).[67]

On the other hand, as stated in section 4.2.1, phosphorescence due to NC_2N (an obvious product of recombining CN radicals) has been detected. The violet band of CN did not noticeably decrease upon annealing, which suggests that only a small fraction of these radicals recombines into cyanogen. The latter is nevertheless easily detected, with an increase of its luminescence after the annealing, and appears also upon a moderate temperature rise, as a thermoluminescent product. A high phosphorescence quantum yield seems to be a crucial parameter responsible for its detection, as well as for the detection of longer chains.

5. CONCLUSIONS

The synthesis of dicyanotriacetylene, induced by the gentle warming of cyanoacetylene/Kr matrixes, the latter solidified in presence of electric discharges (CWRD technique), has been demonstrated. Long linear NC_8N molecules, formed in too low quantities to allow for standard IR-spectroscopic detection, were readily revealed with the electronic luminescence spectroscopy. Phosphorescence of NC_8N, located in the visible range (with an origin around 551 nm) was observed here for the first time; the analysis of its vibronic structure has allowed for measuring the frequencies of g-symmetry vibrational modes.

In previous photochemical studies, it was possible to create HC_5N, NC_4N, and NC_6N *in situ*, from matrix-isolated HC_3N.[14] HC_7N appeared in the course of UV irradiation of $HC_5N\cdots HC_2H$ intermolecular complexes;[13] these seven-carbon chains were thus photochemically produced from appropriately preoriented, neighboring parent species. Our present study involved electric discharges in a gaseous HC_3N/Kr mixture, en route toward its cryogenic trapping. The development of HC_7N and NC_8N bands required the annealing of resultant solid

dx.doi.org/10.1021/jp509908z | J. Phys. Chem. A XXXX, XXX, XXX−XXX

samples, but the bands of products such as NC_4N or NC_6N appeared already in the glow accompanying electric discharges, during the gas solidification (Figure 6, top panel). This suggests that small radical fragments produced in the discharge (e.g., C_3N, C_2H, CN, or C_2) are not the only ones recombining during the cryogenic matrix deposition to form larger molecules; the $NC-(CC)_n^{\bullet}$ and $H-(CC)_n^{\bullet}$ radicals (reaching $n = 2$) are likely to be formed and trapped as well. However, production of the largest species, such as HC_7N or NC_8N, requires an augmented mobility of their direct radical precursors. Obviously, such a mobility increase, introduced by the thermal annealing, affects only the smallest fragments. Among the most important processes responsible for the assembling of NC_8N and HC_7N one can therefore envisage the following:

$$N{\equiv}C{-}(C{\equiv}C)^{\bullet}_{n\leq 2},\ H{-}(C{\equiv}C)^{\bullet}_{n\leq 2} \xrightarrow[\text{annealing}]{CN,C_2,C_2H}$$

$$N{\equiv}C{-}(C{\equiv}C)_{n+1}C{\equiv}N,\ H{-}(C{\equiv}C)_{n+1}C{\equiv}N$$

It should be stressed that the only trace products detected in described experiments are those featuring sufficiently high luminescence quantum yields.

■ ASSOCIATED CONTENT

Supporting Information

Figures S1 and S2 depict the observed spectroscopic details, listed in Table 2. This material is available free of charge via the Internet at http://pubs.acs.org.

■ AUTHOR INFORMATION

Corresponding Author

*M. Turowski. Tel: +48 22 3433353. Fax: +48 22 3433333. E-mail address: mturowski@ichf.edu.pl.

Notes

The authors declare no competing financial interest.

■ ACKNOWLEDGMENTS

The described experiments carried out at the CLUPS laser facility would not have been possible without the help of Dr. C. Jouvet and, especially, Dr. M. Broquier. We have also benefited from the assistance of Dr. S. Boyé-Péronne. We acknowledge the financial support from the National Science Centre (Poland), project No. 2011/03/B/ST4/02763, as well as from the French-Polish programs *Polonium* (2011-2013) and *PICS* (CNRS/PAN; No. 4717).

■ REFERENCES

(1) Turner, B. E. Detection of Interstellar Cyanoacetylene. *Astrophys. J. Lett.* **1971**, *163*, L35.

(2) Dickinson, D. F. Detection of Cyanoacetylene at 18 GHz. *Astrophys. Lett.* **1972**, *12*, 235−236.

(3) McGee, R. X.; Balister, M.; Newton, L. M. Interstellar Cyanoacetylene − J=2→1 J=4→3 Transitions. *Mon. Not. R. Astron. Soc.* **1977**, *180*, 585−592.

(4) Gardner, F. F.; Winnewisser, G. Observations of the J = 1→0 Transitions of the ^{13}C Isotopic Species of Cyanoacetylene (HCCCN) in the Direction of Sagittarius B2. *Astrophys. J.* **1975**, *197*, L73.

(5) Mauersberger, R.; Henkel, C.; Sage, L. J. Dense Gas in Nearby Galaxies. III - HC_3N as an Extragalactic Density Probe. *Astron. Astrophys.* **1990**, *236*, 63−68.

(6) Bockelée-Morvan, D.; Lis, D. C.; Wink, J. E.; Despois, D.; Crovisier, J.; Bachiller, R.; Benford, D. J.; Biver, N.; Colom, P.; Davies, J. K.; et al. New Molecules Found in Comet C/1995 O1 (Hale-Bopp). Investigating the Link between Cometary and Interstellar Material. *Astron. Astrophys.* **2000**, *353*, 1101−1114.

(7) Kunde, V. G.; Aikin, A. C.; Hanel, R. A.; Jennings, D. E.; Maguire, W. C.; Samuelson, R. E. C_4H_2, HC_3N and C_2N_2 in Titan's Atmosphere. *Nature* **1981**, *292*, 686−688.

(8) Bell, M. B.; Feldman, P. A.; Travers, M. J.; McCarthy, M. C.; Gottlieb, C. A.; Thaddeus, P. Detection of $HC_{11}N$ in the Cold Dust Cloud TMC-1. *Astrophys. J. Lett.* **1997**, *483*, L61−L64.

(9) Waite, J. H. J.; Lewis, W. S.; Kasprzak, W. T.; Anicich, V. G.; Block, B. P.; Cravens, T. E.; Fletcher, G. G.; Ip, W.-H.; Luhmann, J. G.; Mcnutt, R. L.; et al. The Cassini Ion and Neutral Mass Spectrometer (INMS) Investigation. *Space Sci. Rev.* **2004**, *114*, 113−231.

(10) Khanna, R. K.; Perera-Jarmer, M. A.; Ospina, M. J. Vibrational Infrared and Raman Spectra of Dicyanoacetylene. *Spectrochim. Acta Part A: Mol. Spectrosc.* **1987**, *43*, 421−425.

(11) Seki, K.; He, M.; Liu, R.; Okabe, H. Photochemistry of Cyanoacetylene at 193.3 nm. *J. Phys. Chem.* **1996**, *100*, 5349−5353.

(12) Coupeaud, A.; Kołos, R.; Couturier-Tamburelli, I.; Aycard, J. P.; Piétri, N. Photochemical Synthesis of the Cyanodiacetylene HC_5N: A Cryogenic Matrix Experiment. *J. Phys. Chem. A* **2006**, *110*, 2371−2377.

(13) Couturier-Tamburelli, I.; Piétri, N.; Crépin, C.; Turowski, M.; Guillemin, J.-C.; Kołos, R. Synthesis and Spectroscopy of Cyanotriacetylene (HC_7N) in Solid Argon. *J. Chem. Phys.* **2014**, *140*, 044329.

(14) Crépin, C.; Turowski, M.; Ceponkus, J.; Douin, S.; Boyé-Péronne, S.; Gronowski, M.; Kołos, R. UV-Induced Growth of Cyanopolyyne Chains in Cryogenic Solids. *Phys. Chem. Chem. Phys.* **2011**, *13*, 16780−16785.

(15) Wu, Y.-J.; Lin, M.-Y.; Chou, S.-L.; Chen, H.-F.; Lu, H.-C.; Chen, H.-K.; Cheng, B.-M. Photolysis of Ethyne in Solid Neon and Synthesis of Long-Chain Carbon Clusters with Vacuum-Ultraviolet Light. *Astrophys. J.* **2010**, *721*, 856.

(16) Smith, A. M.; Agreiter, J.; Bondybey, V. E. Laser-Induced Fluorescence of Matrix-Isolated $HCCCCCN^+$ and $HCCCCCCCN^+$. *Chem. Phys. Lett.* **1995**, *244*, 379−387.

(17) Agreiter, J.; Smith, A. M.; Härtle, M.; Bondybey, V. E. Laser-Induced Fluorescence of Matrix-Isolated $C_4N^+_2$. *Chem. Phys. Lett.* **1994**, *225*, 87−96.

(18) Forney, D.; Freivogel, P.; Fulara, J.; Maier, J. P. Electronic Absorption Spectra of Cyano-substituted Polyacetylene Cations in Neon Matrices. *J. Chem. Phys.* **1995**, *102*, 1510−1514.

(19) Agreiter, J.; Smith, A. M.; Bondybey, V. E. Laser-Induced Fluorescence of Matrix-Isolated $C_6N_2^+$ and of $C_8N_2^+$. *Chem. Phys. Lett.* **1995**, *241*, 317−327.

(20) Grösser, T.; Hirsch, A. Dicyanopolyynes: Formation of New Rod-Shaped Molecules in a Carbon Plasma. *Angew. Chem., Int. Ed. Engl.* **1993**, *32*, 1340−1342.

(21) Schermann, G.; Grösser, T.; Hampel, F.; Hirsch, A. icyanopolyynes: A Homologuous Series of End-Capped Linear sp Carbon. *Chem. − Eur. J.* **1997**, *3*, 1105−1112.

(22) Cataldo, F. Polyynes and Cyanopolyynes Synthesis from the Submerged Electric Arc: About the Role Played by the Electrodes and Solvents in Polyynes Formation. *Tetrahedron* **2004**, *60*, 4265−4274.

(23) Cataldo, F. Polyynes: A New Class of Carbon Allotropes. About the Formation of Dicyanopolyynes from an Electric Arc between Graphite Electrodes in Liquid Nitrogen. *Polyhedron* **2004**, *23*, 1889−1896.

(24) Cataldo, F. Monocyanopolyynes from a Carbon Arc in Ammonia: About the Relative Abundance of Polyynes Series Formed in a Carbon Arc and Those Detected in the Circumstellar Shells of AGB Stars. *Int. J. Astrobiol.* **2006**, *5*, 37−45.

(25) Kołos, R. A Novel Source of Transient Species for Matrix Isolation Studies. *Chem. Phys. Lett.* **1995**, *247*, 289−292.

(26) Miller, F. A.; Lemmon, D. H. The Infrared and Raman Spectra of Dicyanodiacetylene, NCCCCCCN. *Spectrochim. Acta Part A: Mol. Spectrosc.* **1967**, *23*, 1415−1423.

(27) Moureu, C.; Bongrand, J. C. Le Cyanoacetylene C_3NH. *Ann. Chim Paris* **1920**, *14*, 5.

(28) Kołos, R.; Sobolewski, A. L. The Infrared Spectroscopy of HNCCC: Matrix Isolation and Density Functional Theory Study. *Chem. Phys. Lett.* **2001**, *344*, 625−630.
(29) Turowski, M.; Gronowski, M.; Guillemin, J.-C.; Kołos, R. Generation of $HKrC_5N$ and $HXeC_5N$ Molecules. *J. Mol. Struct.* **2012**, *1025*, 140−146.
(30) Frisch, M. J.; Trucks, G. W.; Schlegel, H. B.; Scuseria, G. E.; Robb, M. A.; Cheeseman, J. R.; Montgomery, J. A., Jr.; Vreven, T.; Kudin, K. N.; et al. *Gaussian 03*; Gaussian, Inc.: Wallingford, CT, USA, 2004.
(31) Perdew, J. P.; Ziesche, P.; Eschrig, H. *Electronic Structure of Solids' 91*; Akademie Verlag: Berlin, 1991; Vol. *11*.
(32) Perdew, J. P.; Chevary, J. A.; Vosko, S. H.; Jackson, K. A.; Pederson, M. R.; Singh, D. J.; Fiolhais, C. Atoms, Molecules, Solids, and Surfaces: Applications of the Generalized Gradient Approximation for Exchange and Correlation. *Phys. Rev. B* **1992**, *46*, 6671−6687.
(33) Perdew, J. P.; Chevary, J. A.; Vosko, S. H.; Jackson, K. A.; Pederson, M. R.; Singh, D. J.; Fiolhais, C. Erratum: Atoms, Molecules, Solids, and Surfaces: Applications of the Generalized Gradient Approximation for Exchange and Correlation. *Phys. Rev. B* **1993**, *48*, 4978−4978.
(34) Perdew, J. P.; Burke, K.; Wang, Y. Generalized Gradient Approximation for the Exchange-Correlation Hole of a Many-Electron System. *Phys. Rev. B* **1996**, *54*, 16533−16539.
(35) Burke, K.; Perdew, J. P.; Wang, Y. ectronic Density Functional Theory - Recent Progress and New Direction. *Electronic Density Functional Theory - Recent Progress and New Directions*; Plenum: New York, 1997.
(36) Andersson, M. P.; Uvdal, P. New Scale Factors for Harmonic Vibrational Frequencies Using the B3LYP Density Functional Method with the Triple-Z Basis Set 6-311+G(d,p). *J. Phys. Chem. A* **2005**, *109*, 2937−2941.
(37) Merrick, J. P.; Moran, D.; Radom, L. An Evaluation of Harmonic Vibrational Frequency Scale Factors. *J. Phys. Chem. A* **2007**, *111*, 11683−11700.
(38) Kołos, R.; Waluk, J. Matrix-Isolated Products of Cyanoacetylene Dissociation. *J. Mol. Struct.* **1997**, *408*−*409*, 473−476.
(39) Khriachtchev, L.; Lignell, A.; Tanskanen, H.; Lundell, J.; Kiljunen, H.; Räsänen, M. Insertion of Noble Gas Atoms into Cyanoacetylene: An Ab Initio and Matrix Isolation Study. *J. Phys. Chem. A* **2006**, *110*, 11876−11885.
(40) Guennoun, Z.; Couturier-Tamburelli, I.; Piétri, N.; Aycard, J. P. UV Photoisomerisation of Cyano and Dicyanoacetylene: The First Identification of CCNCH and CCCNCN Isomers − Matrix Isolation, Infrared and Ab Initio Study. *Chem. Phys. Lett.* **2003**, *368*, 574−583.
(41) Kołos, R.; Gronowski, M.; Botschwina, P. Matrix Isolation IR Spectroscopic and Ab Initio Studies of C_3N^- and Related Species. *J. Chem. Phys.* **2008**, *128*, 154305.
(42) Turowski, M.; Gronowski, M.; Boyé-Péronne, S.; Douin, S.; Monéron, L.; Crépin, C.; Kołos, R. The C_3N^- Anion: First Detection of Its Electronic Luminescence in Rare Gas Solids. *J. Chem. Phys.* **2008**, *128*, 164304.
(43) Turowski, M.; Crépin, C.; Gronowski, M.; Guillemin, J.-C.; Coupeaud, A.; Couturier-Tamburelli, I.; Piétri, N.; Kołos, R. Electronic Absorption and Phosphorescence of Cyanodiacetylene. *J. Chem. Phys.* **2010**, *133*, 074310.
(44) Chang, J.-W.; Lee, Y.-P. The C_2N_2 $a\ ^3\Sigma^+_u \rightarrow X\ ^1\Sigma^+_g$ Chemiluminescence in Matrices. *J. Mol. Struct.* **1987**, *157*, 155−165.
(45) Smith, A. M.; Schallmoser, G.; Thoma, A.; Bondybey, V. E. Infrared Spectral Evidence of N≡C−C≡C−C≡C−N≡C: Photoisomerization of N≡C−C≡C−C≡N in an Argon Matrix. *J. Chem. Phys.* **1993**, *98*, 1776−1785.
(46) Turowski, M.; Crépin, C.; Couturier-Tamburelli, I.; Piétri, N.; Kołos, R. Low-Temperature Phosphorescence of Dicyanoacetylene in Rare Gas Solids. *Low Temp. Phys.* **2012**, *38*, 723−726.
(47) Woo, S.-C.; Badger, R. M. The Absorption Spectrum of Cyanogen Gas in the Ultraviolet. *Phys. Rev.* **1932**, *39*, 932−937.
(48) Connors, R. E.; Roebber, J. L.; Weiss, K. Vacuum Ultraviolet Spectroscopy of Cyanogen and Cyanoacetylenes. *J. Chem. Phys.* **1974**, *60*, 5011−5024.
(49) McSwiney, H. D., Jr.; Merritt, J. A. 3100-Å Electronic Absorption of Dicyanodiacetylene. *J. Chem. Phys.* **1970**, *52*, 5184−5186.
(50) Kołos, R. Photolysis of Dicyanodiacetylene in Argon Matrices. *Chem. Phys. Lett.* **1999**, *299*, 247−251.
(51) Turowski, M. Low-Temperature Photochemical and Spectroscopic Studies of the Cyanoacetylenes of Astrophysical Relevance. *Ph.D. dissertation*, Institute of Physical Chemistry, Polish Academy of Sciences, Warsaw, Poland, 2012.
(52) Shimanouchi, T. Tables of Molecular Vibrational Frequencies. Consolidated Volume II. *J. Phys. Chem. Ref. Data* **1977**, *6*, 993−1102.
(53) Wakabayashi, T.; Saikawa, M.; Wada, Y.; Minematsu, T. Isotope Scrambling in the Formation of Cyanopolyynes by Laser Ablation of Carbon Particles in Liquid Acetonitrile. *Carbon* **2012**, *50*, 47−56.
(54) Frosch, R. P. C_2 and C_2^- Spectra Produced by the X Irradiation of Acetylene in Rare-Gas Matrices. *J. Chem. Phys.* **1971**, *54*, 2660−2666.
(55) Fiedler, S. L.; Vaskonen, K. J.; Eloranta, J. M.; Kunttu, H. M. Electronic Spectroscopy of C_2 in Solid Rare Gas Matrixes. *J. Phys. Chem. A* **2005**, *109*, 4512−4516.
(56) Freivogel, P.; Grutter, M.; Forney, D.; Maier, J. P. The $^3\Sigma_u^- \leftarrow X^3\Sigma_g^-$ Electronic Absorption Spectrum of Linear C4 in a Neon Matrix. *Chem. Phys. Lett.* **1996**, *249*, 191−194.
(57) Szczepanski, J.; Ekern, S.; Chapo, C.; Vala, M. Infrared Spectroscopy of Matrix-Isolated Carbon Clusters, with Emphasis on C_8 and C_9. *Chem. Phys.* **1996**, *211*, 359−366.
(58) Withey, P. A.; Shen, L. N.; Graham, W. R. M. Fourier Transform Far Infrared Spectroscopy of a C_4 Bending Mode. *J. Chem. Phys.* **1991**, *95*, 820−823.
(59) Čermák, I.; Förderer, M.; Čermáková, I.; Kalhofer, S.; Stopka-Ebeler, H.; Monninger, G.; Krätschmer, W. Laser-Induced Emission Spectroscopy of Matrix-Isolated Carbon Molecules: Experimental Setup and New Results on C3. *J. Chem. Phys.* **1998**, *108*, 10129−10142.
(60) Szczepanski, J.; Vala, M. The $\nu_1+\nu_3$ Combination Mode of C_3 in Ar and Kr Matrices: Evidence for a Bent Structure. *J. Chem. Phys.* **1993**, *99*, 7371−7375.
(61) Weltner, W., Jr.; McLeod, D., Jr. Spectroscopy of Carbon Vapor Condensed in Rare-Gas Matrices at 4° and 20 K. II. *J. Chem. Phys.* **1964**, *40*, 1305−1316.
(62) Okabe, H. Photodissociation of Acetylene and Bromoacetylene in the Vacuum Ultraviolet: Production of Electronically Excited C_2H and C2. *J. Chem. Phys.* **1975**, *62*, 2782−2787.
(63) Bergeat, A.; Calvo, T.; Dorthe, G.; Loison, J.-C. Fast-Flow Study of the CH + CH Reaction Products. *J. Phys. Chem. A* **1999**, *103*, 6360−6365.
(64) Boyé, S.; Campos, A.; Douin, S.; Fellows, C.; Gauyacq, D.; Shafizadeh, N.; Halvick, P.; Boggio-Pasqua, M. Visible Emission from the Vibrationally Hot C_2H Radical Following Vacuum-Ultraviolet Photolysis of Acetylene: Experiment and Theory. *J. Chem. Phys.* **2002**, *116*, 8843−8855.
(65) Burroughs, A.; Heaven, M. C. Spectroscopy and Relaxation Kinetics of Matrix-Isolated CH/D Radicals. *J. Phys. Chem. A* **2000**, *104*, 3842−3851.
(66) Milligan, D. E.; Jacox, M. E. Spectroscopic Study of the Vacuum-Ultraviolet Photolysis of Matrix-Isolated HCN and Halogen Cyanides. Infrared Spectra of the Species CN and XNC. *J. Chem. Phys.* **1967**, *47*, 278−285.
(67) Bradforth, S. E.; Kim, E. H.; Arnold, D. W.; Neumark, D. M. Photoelectron Spectroscopy of CN^-, NCO^-, and NCS^-. *J. Chem. Phys.* **1993**, *98*, 800−810.